Mineral Res. Exp., Bull., 145, 48-61, 2012

THE CHARACTERIZATION STUDIES OF THE NORTHWEST ANATOLIAN HALLOYSITES/KAOLINITES

Saruhan SAKLAR,* Haşim AĞRILI,* Okan ZİMİTOĞLU,* Bülent BAŞARA* and Uğur KAAN*

ABSTRACT.- The extraction and characterization studies were carried out on representative samples which were taken from iron bearing parts of halloysite, halloysite/kaolin deposits located in the vicinity of Çanakkale and Balıkesir in Northwest Anatolia. Halloysites in these samples are generally in the form of hydro halloysite (10 Å) and kaolinite could also be encountered in some parts. The primary impurities in halloysite and kaolin deposits are limonite (geothite) and muscovite. These deposits might contain quartz, feldspar, gibbsite, smectite group clay minerals and anatase in their structures. The iron content of the clays can be reduced significantly by hydrochloric or oxalic acid treatments. Transmission electron Microscope (TEM) and Scanning Electron Microscope (SEM) analyses on halloysite samples were carried out and it was noticed that halloysite tubes were in cylindrical shape, and in some cases; pores on their surfaces could be observed as a structural feature. In samples studied, tube lengths were measured up to 5 µm by means of SEM analyses, however; TEM analyses have indicated that internal diameters of tubes could decrease down to 5nm and their average diameters ranged in between 40 – 50 nm.

Key words: Halloysite, kaolinite, characterization, leaching.

INTRODUCTION

Halloysite is a double layered aluminosilicate clay is similar to kaolinite but contains cylindrical structures in different nanometer sizes. Diameters of the cylindrical tubes are less than 300 up to 50 µm long. However; their dimensions and shapes could change due to the condition of deposition and formation. Double tubes, structures such as; partly rolled, spherical like, rod like and etc. could also be encountered (Joussein, et al., 2005). Halloysites; as inner sides of their nano tubes are often empty become a subject of investigation in various areas such as; drug, polymer and advanced ceramics (Aguzzi, et al., 2007; Ramirez, et al., 2009; Liu, et al., 2009). There are two different purposes in these investigations. The first is to store special materials into the tubes and the second is to provide stiffening to polymers or ceramics.

Halloysite naturally occurs in two different structures (Churchman, et al., 1972). The first one is the hydrated form which bears water among its layers having a chemical formula of $Al_2Si_2O_5(OH)_4.2H_2O$. The distance between layers is 1 nm (10Å) and is called the "10Å structure". The atomic structure of two molecules of hydrate halloysite ($2\cdot(Al_2Si_2O_5(OH)_4.2H_2O)$) is observed in figure1-a (Murray, 2007). The water between layers withdraws irreversibly in temperatures above 35 -40°C and the interlayer distance decreases to 0.7 nm. 7Å structure is the same as kaolinite. In figure 1b; the XRD pattern for hydrate and dehydrate forms of the halloysite sample between 5°-15° were given which had been taken from the halloysite mine in Balıkesir Gönen region. The dehydrate halloysites could easily be mixed up with kaolinite in XRD analysis, therefore; intercalation methods are necessary for these halloysites to be distinguished by XRD analysis (Joussein, et al., 2007; Nicolini, et al., 2009). Formamide is the first special reagent which transforms dehydrate halloysite into hydrate halloysite (Churchman and Theng, 1984; Churchman et al., 1984; Churchman, 1990). Other reagents such as; dimethyl sulfoxide, potassium acetate, hydrazine could also be used

* Maden Tetkik Arama Genel Müdürlüğü, Jeoloji Etütleri Dairesi, Ankara.

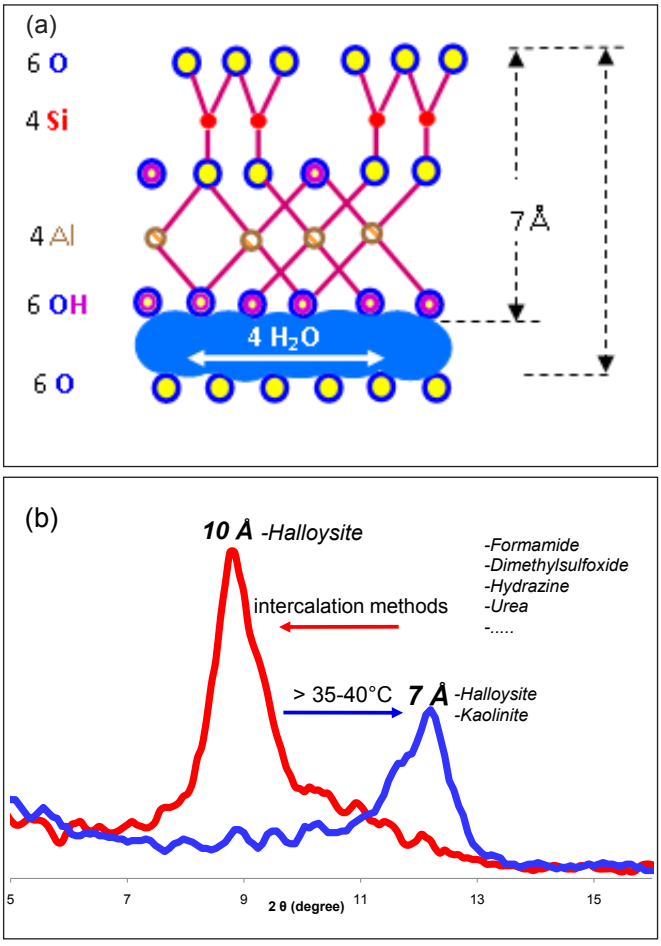

Figure 1- (a) The atomic structure of halloysite (Murray, 2007), (b) XRD pattern (Saklar, 2011*a*).

(Churchman and Carr, 1973; Mellouk, et al., 2009; Horvath, et al., 2011). In order to distinguish halloysites (7Å structure) from kaolinite, the compatibility of methods like XRD, DTA and SEM were investigated and the most accurate result could be achieved by electron microscope (Churchman and Carr, 1975).

Halloysite formations are observed in America, Asia, Africa and Europe, economically important deposits are encountered only in a few countries (Uygun, 1999; Levis and Deasy, 2002). Almost all halloysite world production is provided by New Zealand and shows resemblances with northwestern Anatolian halloysite deposits with respect to the features of formation and mineral contents (Murray, 2007). It was claimed that, northwestern Anatolian halloysite deposits were hydrothermally formed by low pH, silica and aluminum rich solutions (Laçin and Yeniyol, 2006; Ece and Schroeder, 2007). Similar results were also observed in investigations which General Directorate of Mineral Research and Exploration had carried out (Akçay et al., 2008; Dönmez et al., 2008; Duru et al., 2007).

Although halloysites theoretically contain only aluminum, silicate and water (%46.55 SiO_2, %39.49 Al_2O_3, %13.96 H_2O) in their structures (Anthony et al., 1995), Traces of iron, titan, calcium, potassium and sodium may be present. As also seen in table 1, products that have contents close to theoretical values were used in commercial halloysite from New Zelland and Turkey.

Table 1- Commercial product contents of halloysites from New Zelland and Turkey.

	SiO_2	Al_2O_3	Fe_2O_3	TiO_2	CaO	MgO	K_2O	Na_2O	L.O.I
New Zelland	49.50	35.50	0.29	0.09	Trace	Trace	Trace	Trace	13.80
Turkey	46.22	37.30	1.02	0.21	0.26	Trace	0.23	Trace	14.38

In this study, a sequence of enrichment and characterization was carried out on representative samples (Figure 2) taken from iron bearing parts of Balıkesir-Gönen-Alacaoluk (BGL) halloysite deposit, Çanakkale-Yenice-Kırıklar (ÇYK) hallloysite/kaolin deposit and Çanakkale-Gökçeada-Tepeköy (ÇG) kaolin deposits in northwest Anatolia. In addition to removal of iron, it was aimed at producing data by X-ray diffraction (XRD), scanning electron microscope (SEM), energy dispersive X-ray spectrometer point analyses (EDS), transmission electron microscope (TEM) and X-ray fluorescence (XRF) for the description, crystal structure and morphology of clay and accompanying minerals.

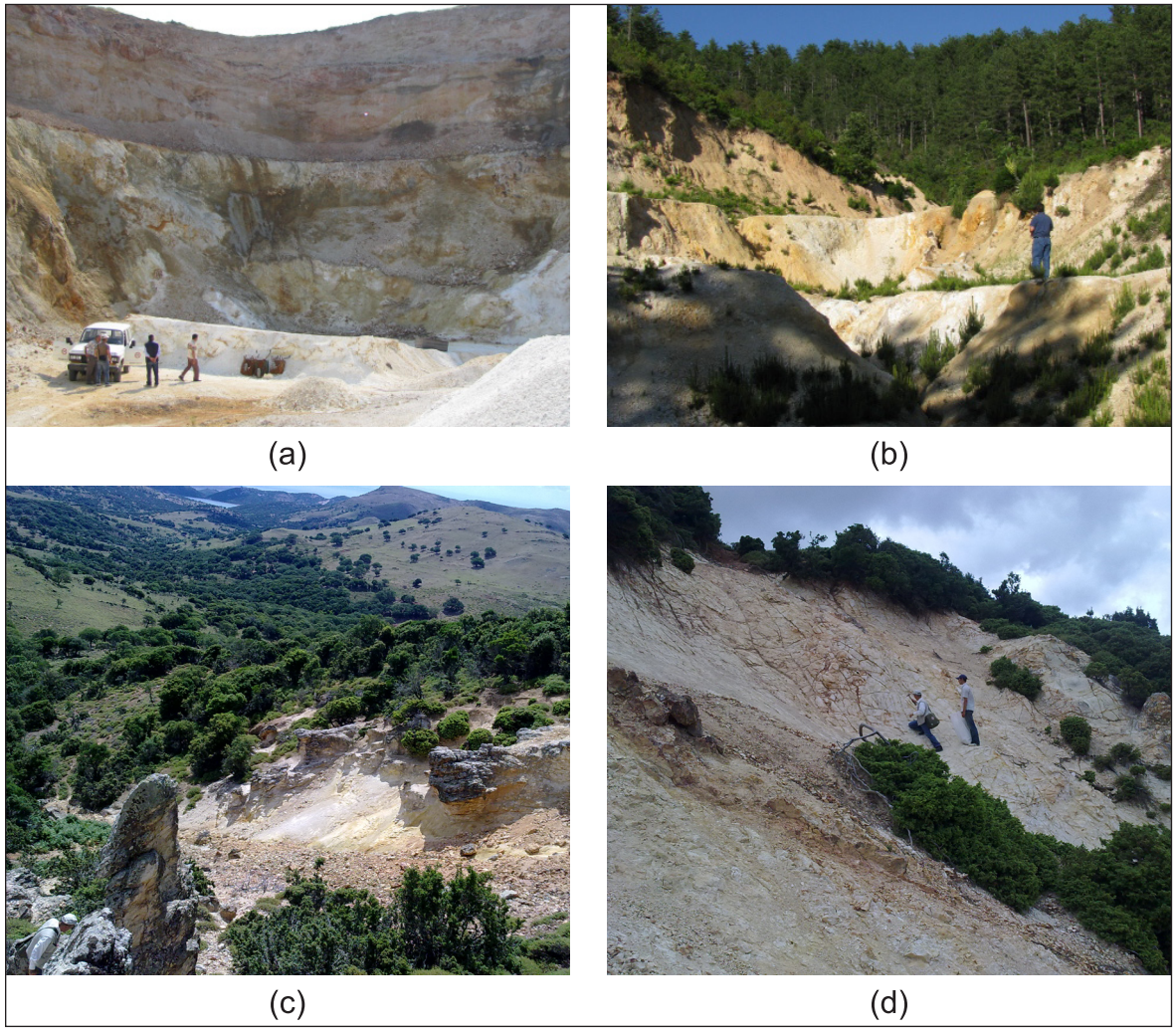

Figure 2- Clay deposits investigated (a): Balıkesir-Gönen-Alacaoluk halloysite deposit; (b): Çanakkale-Yenice-Kırıklar hallloysite/kaolin deposit; (c-d): ÇG: Çanakkale-Gökçeada-Tepeköy kaolin deposit).

GENERAL GEOLOGY

The study area is located in Biga Peninsula in Northwest Anatolia (Figure 3). Pre Tertiary units in Biga Peninsula are observed as tectonic zones trending NE-SW. These zones are the İzmir Ankara zone, Sakarya zone, Çetmi melange and Ezine zone. The Sakarya zone contains Paleozoic and Mesozoic metamorphic units overlain Devonian, Permian, early – late Triassic magmatic, sedimentary and volcanic units.

Ezine zone consists of Late Cretaceous metamorphic units, whereas the Çetmi melange is composed of Maestrichtian – Paleocene flysch and ophiolitic units (Duru et al., 2012).

Tertiary units, however; consist of Eocene to Quaternary sedimentary and volcanic units (Ilgar et al., 2012). Halloysite formations in the region are observed in Paleogene volcanic units composed of andesitic and basaltic lavas and pyroclastics.

Northwest halloysite deposits were typically embedded in partially faulted boundaries between andesitic volcanites and Jurassic dolomite limestones and formed due to the effects of supergene acidic solutions or hypogene hydrothermal solutions on latite and rhyodacite (Uygun, 1999). It was also claimed that halloysites had been formed as a result of hydrothermal effects that were associated with fault zones in low pH environment (2- 3) due to the solution-suspension metasomatism of andesitic tuffs (Erdoğan et al., 2012).

MATERIAL AND METHOD

Hand specimens, collected representatively from iron bearing parts of clay deposits (approximately 100 kg), were kept in between 27 - 29°C temperatures and dried for a few days the preserve the water content between layers. In the next stage; coarse clay pellets were decreased to a size less than 5 mm by conical and roll crushers. To decrease the size was necessary in order to take representative sample and to easily disperse it by water in Denver D-12 flotation cell. The dispersion was made by batch experiments in every 30 min intervals at 15-20% solid ratio. The dispersed clay was then prepared at different fractions by wet sieving.

Figure 3- Location map.

Chemical analyses were carried out for whole rock sample and grain size fractions. In terms of clay content, it was noticed that the ÇG sample was condensed at a size finer than 10 µm and test samples were prepared by wet sieving in this size. However; test samples were prepared carrying out wet sieving at 90 µm which was relatively a coarse size as there had been no fractional differentiations in BGL and ÇYK samples. Water in clay samples that had been wet sieved was then drained out, oven dried and the dry pellets were then disintegrated by short grinding. Representative homogenous clay samples in dry and powder forms were obtained for each clay beds (Saklar, 2011*a*).

In order for clay contents of samples to be more sensitively studied by XRD analysis, parts of whole rock samples finer than 2 µm were prepared by decantation method using Stokes' equation (Wills, 2006).

Chemical analyses, on the other hand, were carried out by using Philips Axios XRF spectrometry. XRD analyses were performed by Bruker D8 Advance X Ray diffractometer using Cu-Kα radiation, at 2 -70° 2θ interval, 40 kV resistance and at a current of 40 mA. Scanning Electron Microscope (SEM) analyses were performed by FEI Quanta 400 MK2 instrument on gold/palladium coated samples. 300 kV FEI Tecnai G2 F30 model Transmission Electron Microscope (TEM) were used in order to analyze crystal morphologies of the samples. Samples were dispersed by ultrasonic bath in ethanol before analysis and the ethanol was evaporated in open air.

To detect coloring minerals in samples by XRD analysis, tests were made by wet magnetic separator with high field strength (Master Magnet 500) under a magnetic field of 20,000 Gauss. Nevertheless; no result has been obtained in BGL and in ÇG samples, but a very little magnetic fraction in ÇYK sample. Therefore; samples necessary for XRD analyses of coloring minerals were obtained by chiseling with a needle from brown/red colored parts of hand specimens (Figure 4).

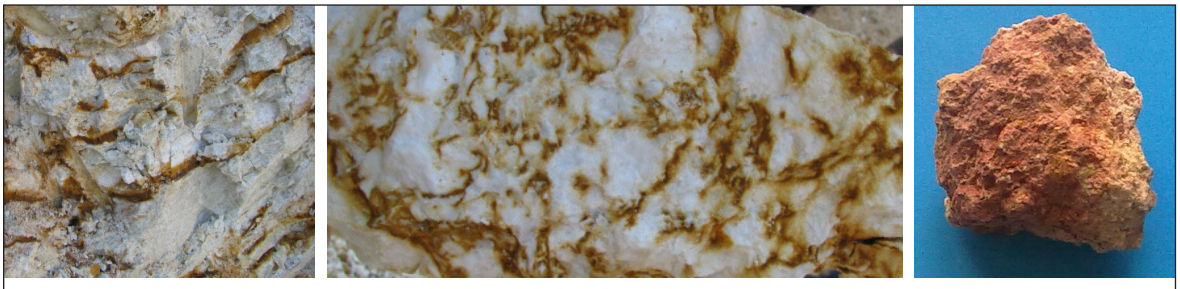

Figure 4- Hand specimens containing coloring minerals in (a) ÇYK, (b) BGL and (c) ÇG samples (dark areas indicate iron oxide/hydroxide colorings on samples).

Characterization experiments, in addition to whole rock samples, were performed also on samples which had been cleaned by extraction experiments. Fe_2O_3 contents of the whole rock samples were extracted using hydrochloric and oxalic acid (HCl ve $(COOH)_2$) at specific time (150 min), temperature (80°C) and concentration values (Table 2) (Saklar, 2011*a*).

Table 2- Concentration values used in extraction

Sample	Molarity (M)	
	HCl	$(COOH)_2$
ÇYK	1.17	0.59
ÇG	0.84	0.42
BGL	1.28	0.84

Solid/liquid mixtures containing 10% solid in weight which had been prepared with distilled water then kept for 10 minutes were used to measure the pH values of samples, (TS2326, 1997).

FINDINGS

Natural pH, density and chemical content values of whole rock samples were presented in tables 3 and 4, and their related XRD results were given in figure 5. Each of the three clay samples is acidic in character and their pH and density values do not show much difference with their sizes (Table 3). ÇG sample have lower pH and higher density values compared to other samples. The reason for having the high density originates from much silicate content in ÇG sample.

Table 3- Density and pH values of whole rock samples

Sample	BGL		ÇG		ÇYK	
	Whole rock sample	<90 µm	Whole rock sample	<10 µm	Whole rock sample	<90 µm
Density	2.50	2.50	2.63	2.60	2.47	2.48
pH	4.80	4.85	3.50	3.70	4.15	4.10

Table 4- Chemical contents of whole rock samples

Sample	SiO_2	Na_2O	MgO	Al_2O_3	P_2O_5	K_2O	CaO	TiO_2	Fe_2O_3	SO_3	L.O.I.
BGL (whole rock sample)	44.14	0.08	0.21	37.66	0.15	0.21	0.02	0.09	2.05	0.12	15.10
BGL (<90 µm)	44.53	0.07	0.21	37.53	0.16	0.22	0.05	0.12	2.10	0.14	14.65
ÇG (whole rock sample)	66.51	0.23	0.82	18.00	0.15	3.50	0.08	0.58	2.17	1.59	6.10
ÇG (<10 µm)	60.84	0.18	0.92	22.15	0.18	3.78	0.10	0.58	2.14	1.55	7.30
ÇYK (whole rock sample)	43.77	<0.01	0.41	34.82	0.69	0.36	0.16	0.35	3.33	0.36	15.20
ÇYK (<90 µm)	43.55	<0.01	0.48	35.34	0.74	0.37	0.18	0.43	3.58	0.39	14.65

*MnO was detected in trace amount.

The chemical content of BGL sample is very close to the theoretical content of halloysites but contains 2% Fe_2O_3. Results of the chemical analyses of the portion finer than 90 µm in width are almost the same as the whole rock sample. XRD results also show that BGL sample is a pure hydrate halloysite. During tests run both for the whole rock sample and for <2 µm, regular halloysite peaks were obtained; besides, a very large 10Á peak at <2 µm fraction was obtained (Figure 5 a, b). In Figures 5c and 5d, it is seen that hydrate halloysites turned into dehydrate (7Á) structure as these were dried up (>60°C) after being extracted by HCl and $(COOH)_2$. Traces of crystobalite were rarely seen to accompany the halloysite.

XRD analysis for ÇYK sample without dehydration showed clear 10Á halloysite and 7Á kaolinite peaks (Figure 5a). In Table 4, there was not found any serious chemical difference between the whole rock sample and <90 µm portion. The 10Á peak intensity in <2 µm fraction is more than that of the whole rock sample. However; 7Á kaolinite peak in <2 µm fraction is less than the whole rock sample. Therefore halloysite ratio in ÇYK sample is relatively higher than that of kaolinite. Since HCl and $(COOH)_2$ samples of dehydrated halloysites give only 7Á peak, the peaks in diffractograms were detected as halloysite+kaolinite. This phenomenon indicates how significant the intercalation is for the detection of dehydrated halloysites by XRD method and the importance of preservation of

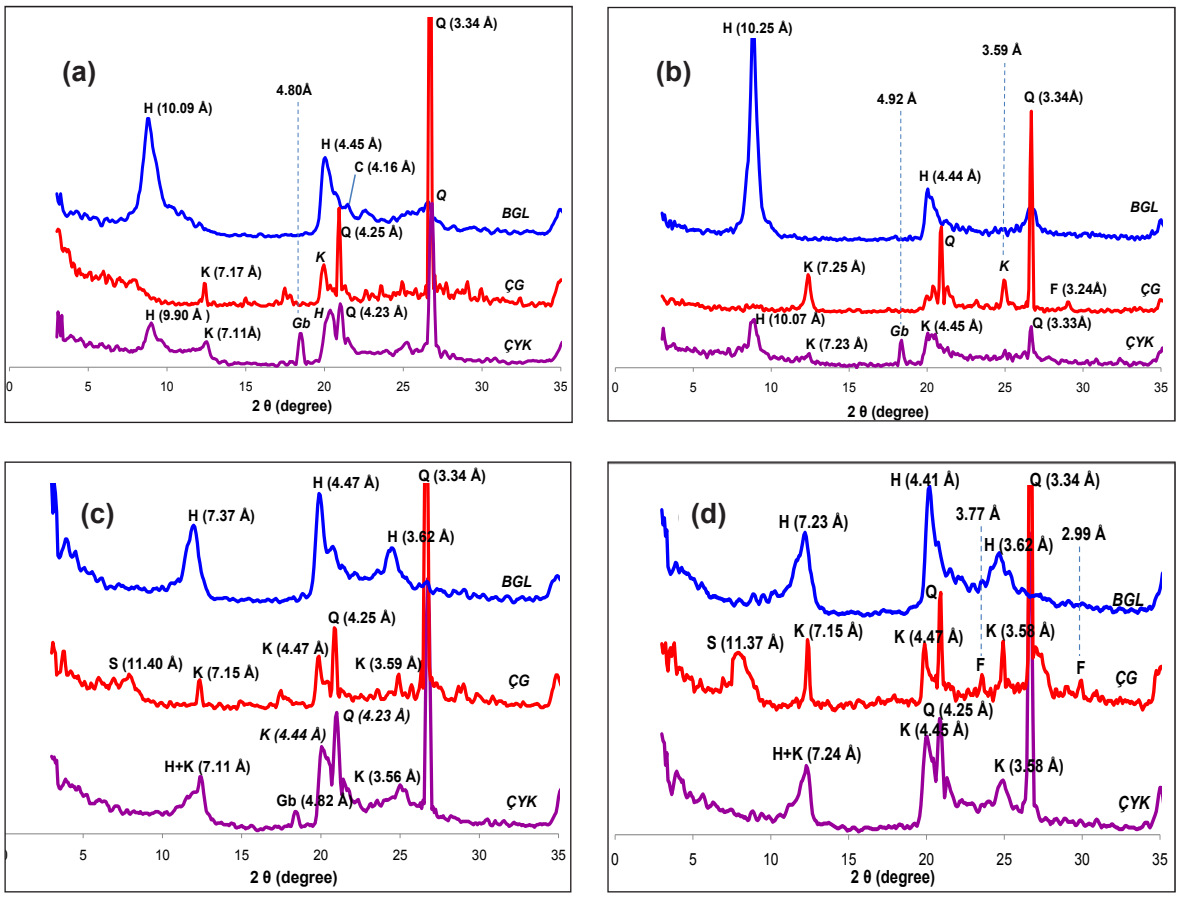

Figure 5- XRD diffractograms of (a) whole rock sample, (b) <2 μm fraction, (c) HCl extraction product, (d) (COOH)2 extraction product (H: halloysite, Q: quartz, C: crystobalite, S: smectite clay group, F: feldspar, Gb: gibbsite)

the hydrate form Gibbsite was detected in the whole rock sample and in XRD analyses of <2 μm and HCl concentrate.

The ÇG sample, in addition to kaolinite peaks, gives a classically silicified kaolinite XRD pattern with broader quartz peak with respect to BGL and ÇYK. Despite the weak kaolinite peak obtained in the whole rock sample, a relatively broader kaolinite peak was detected in the <10 μm fraction. Chemical analysis results support this. Fire loss, alumina and silica ratios indicate that the <10 μm portion contains more kaolinite (Table 4). Similar results were frequently seen in silicified kaolin deposits (Saklar, 2011*a*).

The chemical contents of extraction products obtained for size fractions of whole rock samples were given in Table 5 and 6. It was observed that HCl or $(COOH)_2$ extraction processes cause a decrease in Fe_2O_3 content of all samples especially the BGL. Decreasing Al_2O_3 proportions in BGL and ÇYK samples indicate that these caused Al^{+3} ions at high temperature to dissolve. As a result, the decrease in Al_2O_3 content caused a spontaneous increase in SiO_2 content as Si/Al ratio increased. The rea-

sons why this result has not been taken in ÇG sample is the use of less acidic concentration and less consistence of clay relative to other samples.

The extraction process does not cause a change in crystal structure as seen in XRD results in figure 4. Differences in the crystal structure form only at very high acidic concentrations (>3M) and a transformation into amorphous structure could occur (Mako, et al., 2006; Panda et al., 2010).

Table 5- Concentration contents of HCl extraction experiments

Sample	SiO_2	Na_2O	MgO	Al_2O_3	P_2O_5	K_2O	CaO	TiO_2	Fe_2O_3	SO_3	L.O.I.
BGL	48.63	<0.01	0.19	35.59	0.03	0.22	0.02	0.12	0.17	0.03	14.88
ÇG	64.32	0.16	0.88	22.80	0.13	4.02	0.08	0.67	0.43	0.50	5.75
ÇYK	54.86	<0.01	0.47	30.53	0.10	0.44	0.15	0.49	1.07	0.05	11.65

Table 6- Concentration contents of (COOH)2 extraction experiments

Sample	SiO_2	Na_2O	MgO	Al_2O_3	P_2O_5	K_2O	CaO	TiO_2	Fe_2O_3	SO_3	L.O.I.
BGL	55.51	<0.01	0.19	29.22	0.02	0.24	0.03	0.14	0.16	0.03	14.35
ÇG	65.53	0.18	0.84	21.28	0.12	3.97	0.09	0.70	0.38	0.54	6.10
ÇYK	52.99	<0.01	0.50	30.24	0.08	0.42	0.12	0.51	0.98	0.06	13.82

XRD analyses of samples prepared in order to understand the coloring minerals were given in figure 6. Limonite (Geothite) could be detected in all samples even at small peaks. Again, small peaks of muscovite were observed in ÇYK and BGL samples. Feldspar as the alkaline source was detected in ÇG sample. Since TiO_2 encountered in chemical analyses were at very low proportions, it could not be detected which mineral it had been originated from in XRD anal-

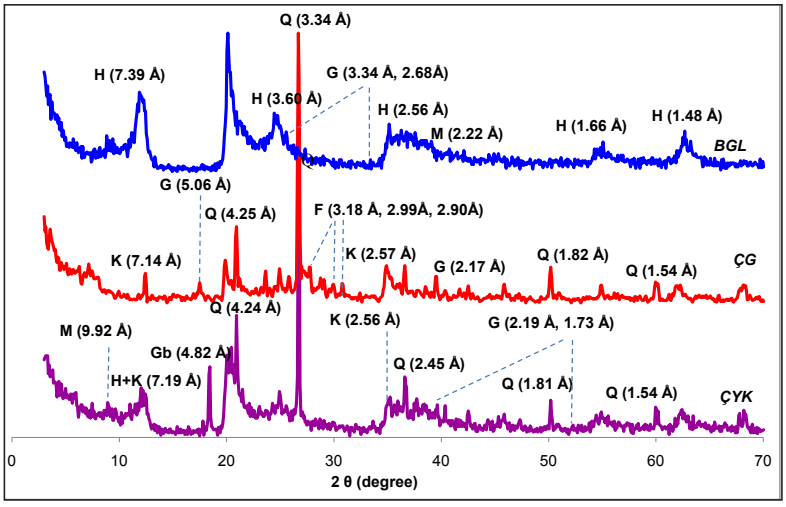

Figure 6- XRD diffractograms belonging to coloring minerals (H: halloysite, K: kaolinite, Q: quartz, G: goethite, M: muscovite F: feldspar, G: gibbsite).

ysis because XRD method can not detect minerals that have proportions less than 5% (Saka, 1997). Nonetheless; previous studies carried out at another Balıkesir – Gönen halloysite deposit with sulphur which has relatively higher TiO_2 proportion indicated that TiO_2 source were anatase mineral, and vermiculite could accompany in some cases (Saklar et al., 2010; Saklar, 2011*a*).

Results of scanning electron microscope (SEM) confirm XRD results (Figure 7). It is understood that BGL sample was halloysite that formed completely as cylindrical tubes. Cylinders have regular and homogenous size distributions. In all portions of ÇG sample in which the analysis had been performed, classical kaolinite plates were observed in a couple of µm sizes. As for the ÇYK sample, halloysite tubes were observed between kaolinite plates. It is not possible to understand the halloysite kaolinite proportion in a sample by electron microscope; however, this proportion could be understood by intercalation using XRD method (Joussein, et al., 2007).

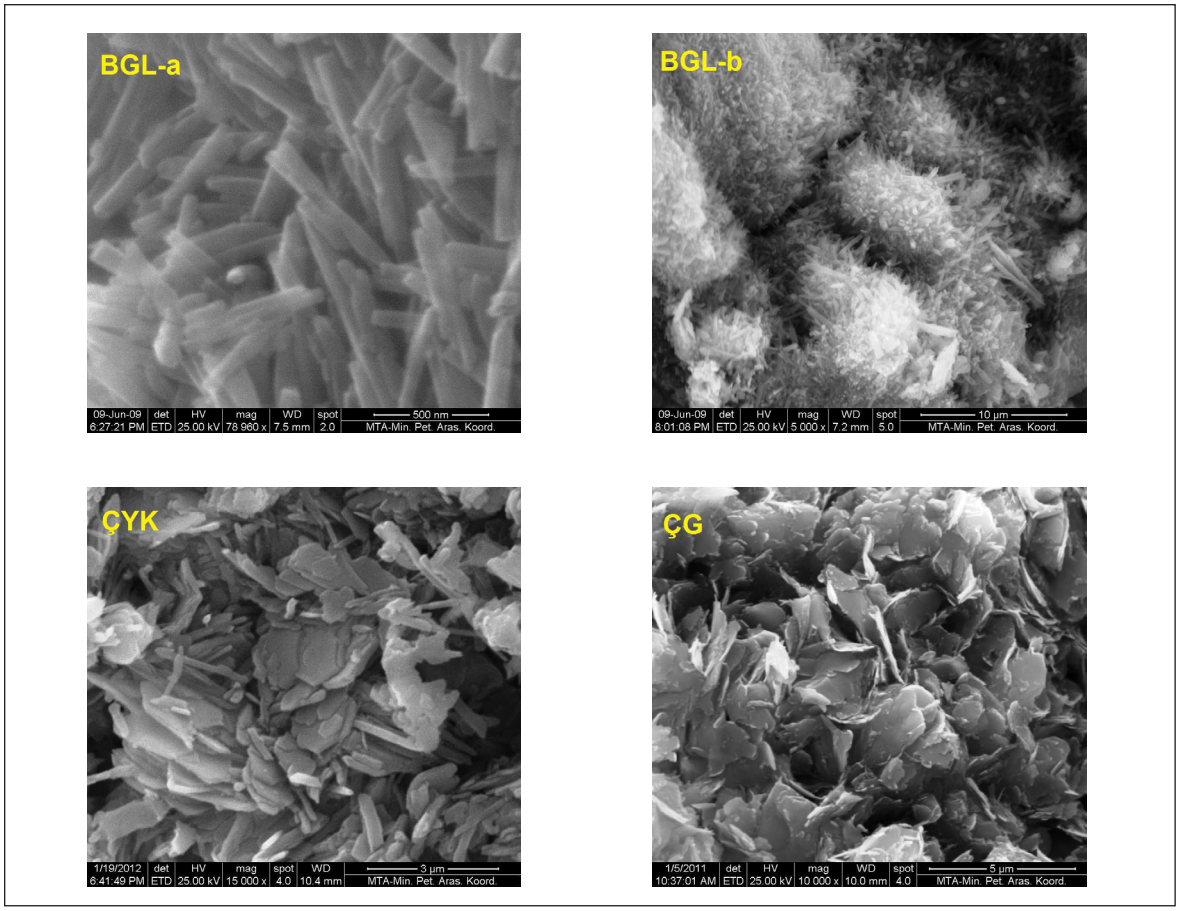

Figure 7- Scanning electron microscope views of Gönen, Yenice and Gökçeada samples (BGL-a: tubular halloysite crystals; BGL-b: pelleted tubular halloysite crystals; ÇYK: Tubular halloysite crystals between and on sheet like kaolinite crystals; ÇG: Sheet like kaolinite crystals)

In figure 8, very tiny iron oxide pellets, in ÇYK sample, are observed. EDS point analysis data also indicate that these are iron oxide, but the results are insufficient to understand with which mineral these iron oxides might be associated. XRD results shown in figure 6, indicate that these are goethite mineral. Tiny iron oxide/hydroxide pellets detected by SEM method in ÇYK sample could not be monitored by SEM although they were detected by the results of XRD and EDS analyses. It might be due to that, iron oxide/hydroxide minerals, in the form of extremely fine grained particles in submicron size, might have remained among clay minerals or attached to halloysite tubes –kaolinite plates.

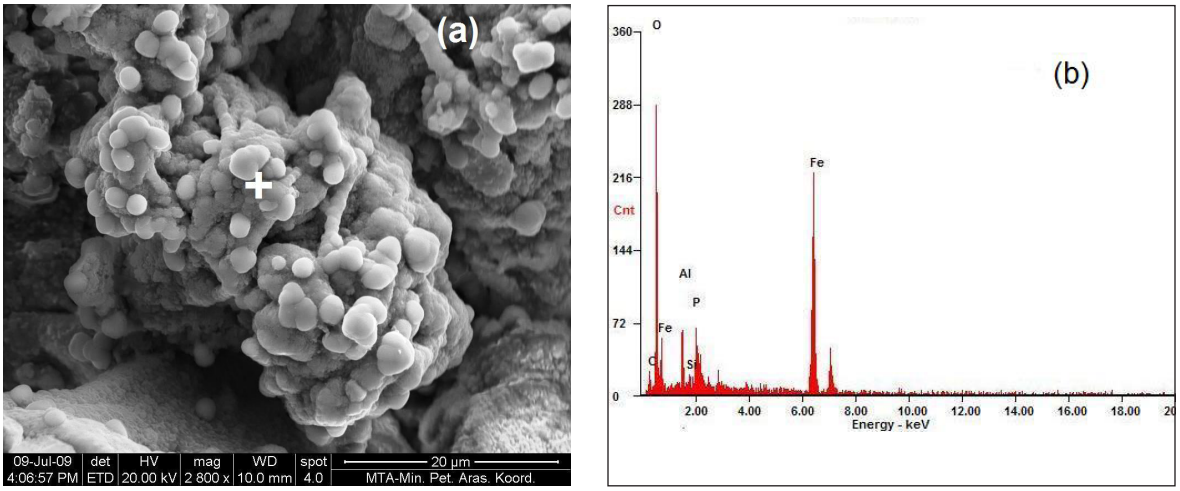

Figure 8- Electron microscope view of iron oxide/hydroxide minerals in ÇYK sample ((a): +: point of EDS analysis) and (b): graph of EDS point analysis).

TEM analyses were performed in order to investigate the morphology of tubes on BGL sample which is a characteristic halloysite. It was also noticed that almost all halloysite grains were in the form of cylindrical tubes and inner sides of cylinders were mostly empty. It was observed that diameters of tubes in investigated samples had decreased down to 5 nm and averaged between 40 -50 nm. It was found that the length of tubes in some samples could be up to 5 µm in SEM analysis (Figure 7). However; shorter tube lengths were detected by TEM results (Figure 9, 10). Pores on cylindrical tubes were detected independent from being hydrate/dehydrate of the sample (Figure 9 b, e) (Churchman, et al., 1995).

TEM analyses were performed also on HCl and $COOH_2$ concentrates which were obtained by the extraction process and were given in figure 10. It is seen that, tube views obtained are more accurate, and cylindrical tubes were not affected by high temperature (80ºC) and by concentrated acid solutions. There are some pores on tubes and their resemblances are present in native forms of samples as seen in Figure 9. So; it is thought that these pores were originated from acid treatment.

DISCUSSION AND CONCLUSIONS

Characterization studies were made for halloysite, kaolin/halloysite and kaolin deposits observed in Çanakkale-Balıkesir vicinities in northwestern Anatolia. Halloysites of the region are in the form of hydrohalloysite (10 Å) as it is in Balıkesir – Gönen (BGL) sample, and kaolinite could also enter their structures as it occurred in Çanakklae – Yenice (ÇYK) sample. When similarities in formational and mineralogical features are taken into consideration, it could be said that

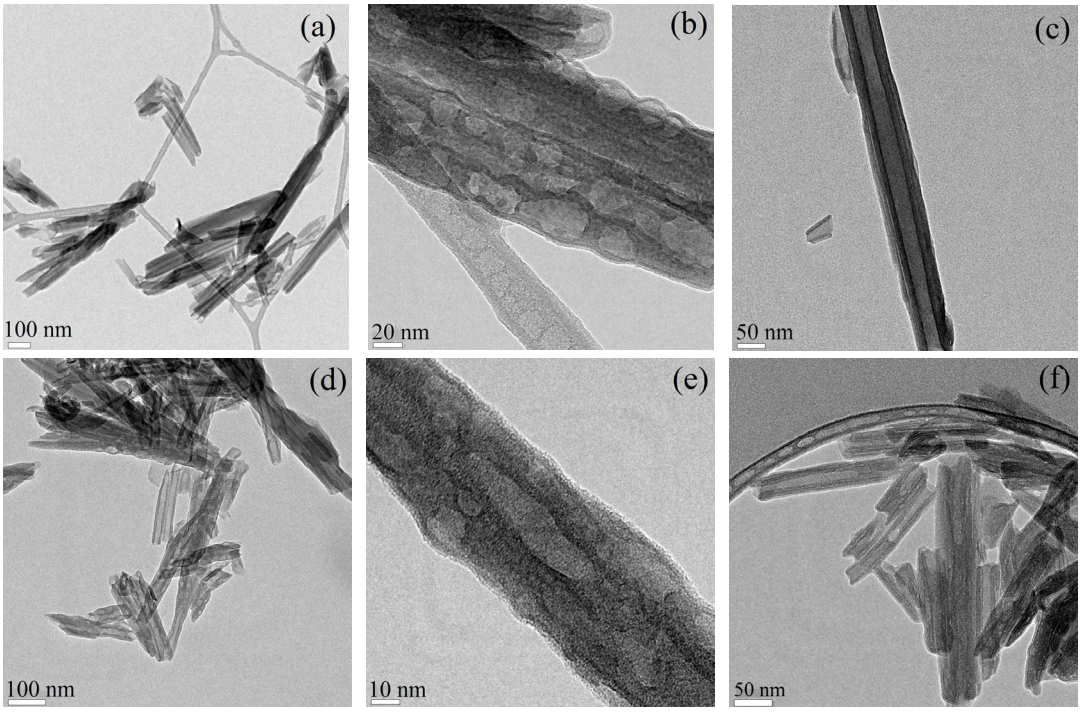

Figure 9- (a), (b), (c): hydrate; (e), (f), (g): dehydrate halloysite TEM views of the BGL sample.

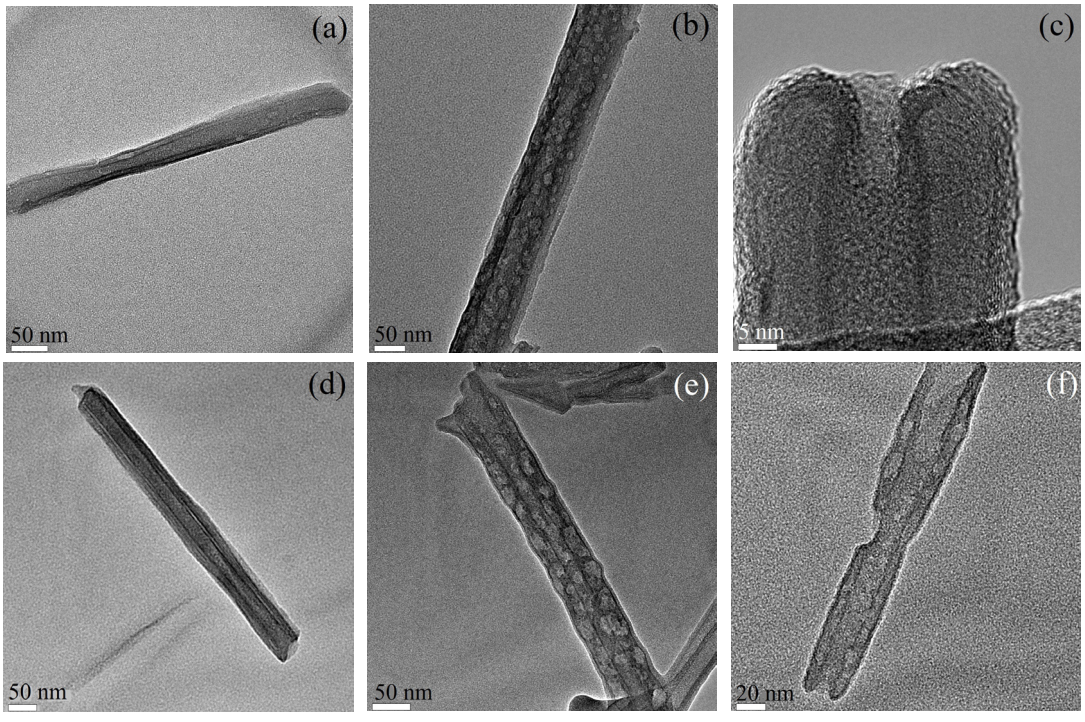

Figure 10- TEM views of extraction concentrates of HCl (a, b, c) and $(COOH)_2$ (d, e, f) for BGL halloysite sample.

there is a possibility of occurrence of halloysite in other kaolin deposits present in northwest Anatolia.

In order to fully understand the differentiation of halloysite/kaolinite, the use of an electron microscope is necessary. However; XRD analysis is preferred as it is simpler and a more general method to apply in clay mineralogy. The application of the intercalation method is necessary in XRD analysis if halloysite loses water between its layers, because the halloysite mineral in dehydrate structure gives the same peak value as kaolinite 7Å (001). The necessity of intercalation in XRD method appears when interlayer waters are lost in temperatures above 40ºC and easily turns into dehydrate structure.

Deposits in the region show similarities also in terms of coloring minerals that they contain. If goethite (limonite) which was detected as the primary contaminant is in thin dimension, it has a strong coloring effect in clay deposits. The anatase that had been detected in previous studies in very close clay deposits (BGL 100 m) is considered also to be the source of TiO_2 in studied deposits. Gibbsite and smectite were also encountered sometimes.

Northwest Anatolian halloysites are chemically very close in content with that of New Zealand halloysites. It was investigated that diameters of cylinders could decrease to 5 nm but are 40 -50 nm in average in studied samples. Tubes which could reach 5 µm in length by SEM analyses were detected less than 1µm in others by TEM analyses.

Another significant finding is that the halloysite tubes were not affected by the treatment of concentrated acid (1.28M HCl and 0.84M (COOH)2) at high temperature (80°C) in long time period (2.5 hours). In spite of the fact that some pores were detected in tubes by TEM analyses, it was also determined that these pores had been in their unprocessed and in native forms.

ACKNOWLEDGEMENT

We would like to thank to geological engineer Baki Günaydın and geological engineer Turgut Çolak and to all MTA staffs, Bilkent UNAM, Kalemaden and to ESAN.

The manuscript received on March 5, 2012.

REFERENCES

Aguzzi, C., Cerezo, P., Viseras, C. and Caramella C. 2007. Use of clays as drug delivery systems: possibilities and limitations. Applied Clay Science, 36, 22-36.

Anthony, J.W., Bideaux, R.A., Bladh, K.W. and Nichols, M.C., 1995. Handbook of Mineralogy, Vol. II. Silica, Silicates, Mineral Data Publishing, Tucson, Arizona.

Akçay, A.E., Dönmez, M., Ilgar, A., Duru, M. and Pehlivan, Ş. 2008. 1:100.000 ölçekli Türkiye jeoloji haritaları, Bandırma H 19 paftası No 103, Maden Tetkik ve Arama Genel Müdürlüğü, 26 s. Ankara.

Churchman, G. J. 1990. Relevance of different intercalation tests for distinguishing halloysite from kaolinite in soils. Clays and Clay Minerals, 38, 591–599.

_____, Aldridge, L. P. and Carr, R. M. 1972. The relationship between the hydrated and dehydrated states of an halloysite. Clays and Clay Minerals, 20, 241-246.

_____ and Carr, R. M. 1973. Dehydration of the washed potassium acetate complex of halloysite. Clays and Clay Minerals, 21, 423-424.

_____ and _____ 1975. The definition and nomenclature of halloysites. Clays and Clay Minerals, 23, 382-388.

_____ and Theng, B. K. G. 1984. Interactions of halloysites with amides: mineralogical factors affecting complex formation. Clay Minerals, 19, 161-175.

_____, Whitton, J. S., Claridge, G. G. C. and Theng, B. K. G. 1984. Intercalation method using formamide for differentiating halloysite from kaolinite. Clays and Clay Minerals, 32, 241–248.

Churchman, G. J., Davy, T. J., Aylmore, L. A. G., Gilkes, R. J. and Self, P. G. 1995. Characteristics of fine pores in some halloysites. Clay Minerals, 30, 89–98.

Dönmez, M., Akçay, A.E., Duru, M., Ilgar, A. and Pehlivan, Ş. 2008. 1:100.000 ölçekli Türkiye jeoloji haritaları, Çanakkale H 17 paftası No 101, Maden Tetkik ve Arama Genel Müdürlüğü, 27 s. Ankara.

Duru, M., Pehlivan, Ş., Okay, A.İ., Şentürk, Y. and Kar, H.,2012. Biga Yarımadası'nın Tersiyer Öncesi Jeolojisi, s.7-74, Biga Yarımadası'nın Genel ve Ekonomik Jeolojisi, Editörler: Erdoğan Yüzer, Gürkan TUNAY, MTA Özel Yayın Serisi, No: 28, Ankara

_____, _____, Dönmez, M., Ilgar, A. and Akcay, A.E. 2007. 1:100.000 ölçekli Türkiye jeoloji haritaları, Bandırma H 18 paftası No 102, Maden Tetkik ve Arama Genel Müdürlüğü, 50 s. Ankara.

Ece, Ö. İ. and Schroeder, P. A. 2007. Clay mineralogy and chemistry of halloysite and alunite deposits in the Turplu area-Balıkesir-Turkey. Clays and Clay Minerals, 55, 1, 18-35.

Erdoğan, M., Gençoğlu, H. and Mahmutoğlu, Y., 2012. Biga Yarımadası'nın Endüstriyel Hammadde Olanakları, s.273-289, Biga Yarımadası'nın Genel ve Ekonomik Jeolojisi, Editörler: Erdoğan Yüzer, Gürkan Tunay, MTA Özel Yayın Serisi, No: 28, Ankara

Horvath, E., Kristof, J., Kurdi, R., Mako, E. and Khunova, V. 2011. Study of urea intercalation into halloysite by thermoanalytical and spectroscopic techniques. Journal of Thermal Analysis and Calorimetry, 105, 53–59

Ilgar, A., Demirci, E.S. and Demirci, Ö., 2012. Biga Yarımadası Tersiyer İstifinin Stratigrafisi ve Sedimantolojisi, s.75-122, Biga Yarımadası'nın Genel ve Ekonomik Jeolojisi, Editörler: Erdoğan Yüzer, Gürkan Tunay, MTA Özel Yayın Serisi, No: 28, Ankara Imerys Minerals Ltd. 2012, Technical Data Sheet, NZCC, http://www.imerys-ceramics.com/Upload/Fichiers/Halloysite_table1.pdf

Joussein, E., Petit, S., Churchman, G. J, Theng, B. K. G., Righi, D. and Delvaux, B. 2005. Halloysite clay minerals-a review. Clay Minerals, 40, 383–426.

_____, _____ and Delvaux, B. 2007. Behavior of halloysite clay under formamide treatment. Applied Clay Science, 35, 17–24.

Kalemaden, 2012. Kaolinitler Kataloğu, Ürün no:151, http://www.kalemaden.com.tr/kaolinit.pdf

Lacin, D. and Yeniyol, M. 2006. An example to the halloysite deposits formed associated with the andesitic pyroclastics: Soğucak halloysite deposit (Yenice-Çanakkale). Istanbul Üniv. Yerbilimleri Journal, 19, 1, 27-41.

Levis, S. R. and Deasy, P. B. 2002. Characterisation of halloysite for use as a microtubular drug delivery system. Int. J. of Pharmaceutics, 243, 1-2 ,125-134.

Liu, M., Guo, B., Du, M., Chen, F. and Jia, D. 2009. Halloysite nanotubes as a novel nucleating agent for isotactic polypropylene. Polymer, 50, 3022–3030.

Mako, E., Senkar, Z., Kristof, J. and Vagvölgyi, V., 2006. Surface modification of mechanochemically activated kaolinites by selective leaching, Journal of Colloid and Interface Science, 294, 362–370.

Mellouk, S., Cherifi, S., Sassi, M., Marouf-Khelifa, K., Bengueddach, A., Schott, J. and Khelifa, A. 2009. Intercalation of halloysite from Djebel Debagh (Algeria) and adsorption of copper ions. Applied Clay Science, 44, 230–236.

Murray, H. H. 2007. Applied Clay Mineralogy- Developments in Clay Science 2. Elsevier, 180p.

Nicolini, K. P., Fukamachi, C. R. B., Wypych, F. and Mangrich, A. S. 2009. Dehydrated halloysite intercalated mechanochemically with urea: thermal behavior and structural aspects. Journal of Colloid and Interface Science, 338, 474–479.

Panda, A.K., Mishraa, B.G., Mishrac,D.K. and Singha, R.K., 2010. Effect of sulphuric acid treatment on the physico-chemical characteristics of kaolin clay", Colloids and Surfaces A: Physicochem. Eng. Aspects, 363, 98-104.

Ramirez, S. B., Fernandez, E. V. R, Albero, J. S., Escribano, A. S., Blas, M. M. P. and Montiel, A. G. 2009. Use of nanotubes of natural halloysite as catalyst support in the atom transfer radical polymerization of methyl methacrylate, Microporous and Mesoporous Materials, 120, 132–140.

Saka, A.H. 1997. Mineralojik analizlerde X-Işını toz kırınım yönteminin temel prensipleri ve laboratuar şartlarının standardizasyonu. MTA Yayını, 234 s.

Saklar, S. 2011*a*. Türkiye halloysit kaynaklarının değerlendirme olanaklarının araştırılması proje sonuç raporu, Maden Tetkik Arama Genel Müdürlüğü Rapor No: 11467, 122 s. Ankara.

Saklar, S., Ağrılı, H., Köse, A., Zimitoğlu, O. and Aygün, A. 2010. Beneficiation of pyritic halloysite from northwestern Turkey. XIIth International Mineral Processing Symposium, 6-8 October 2010, Cappadocia, 783-792.

TS2326, Türk Standartları, 1997. Pigmentler ve dolgu malzemeleri için genel deney metotları, Kısım-9: sulu süspansiyonun pH değeri tayini, TSE, Ankara.

Uygun, A. 1999. KB - Anadoluda karbonat kayaları içine yerleşmiş bazı halloysit yataklarının jeolojisi ve oluşumu. MTA Dergisi, 121, 141-151.

Wills, B. A. 2006, Wills' Mineral Processing Technology: an introduction to practical aspects of ore treatment and mineral recovery. Elsevier, 441p.